JCTC Journal of Chemical Theory and Computation

Article

pubs.acs.org/JCTC

Sensitivity of ab Initio vs Empirical Methods in Computing Structural Effects on NMR Chemical Shifts for the Example of Peptides

Chris Vanessa Sumowski,[†] Matti Hanni,[†,‡] Sabine Schweizer,[†] and Christian Ochsenfeld*[,†]

[†]Chair of Theoretical Chemistry, Department of Chemistry, University of Munich (LMU), Butenandtstr. 7, D-81377 Munich, Germany and Center for Integrated Protein Science (CIPSM) at the Department of Chemistry, University of Munich (LMU), Butenandtstr. 5-13, D-81377 Munich, Germany

Supporting Information

ABSTRACT: The structural sensitivity of NMR chemical shifts as computed by quantum chemical methods is compared to a variety of empirical approaches for the example of a prototypical peptide, the 38-residue kaliotoxin *KTX* comprising 573 atoms. Despite the simplicity of empirical chemical shift prediction programs, the agreement with experimental results is rather good, underlining their usefulness. However, we show in our present work that they are highly insensitive to structural changes, which renders their use for validating predicted structures questionable. In contrast, quantum chemical methods show the expected high sensitivity to structural and electronic changes. This appears to be independent of the quantum chemical approach or the inclusion of solvent effects. For the latter, explicit solvent simulations with increasing number of snapshots were performed for two conformers of an eight amino acid sequence. In conclusion, the empirical approaches neither provide the expected magnitude nor the patterns of NMR chemical shifts determined by the clearly more costly ab initio methods upon structural changes. This restricts the use of empirical prediction programs in studies where peptide and protein structures are utilized for the NMR chemical shift evaluation such as in NMR refinement processes, structural model verifications, or calculations of NMR nuclear spin relaxation rates.

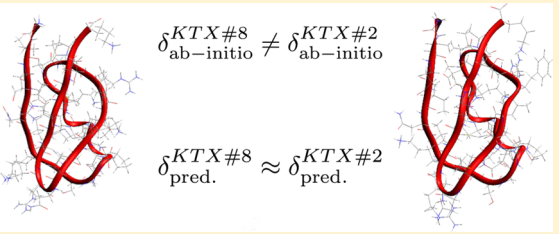

1. INTRODUCTION

Over the last decades, nuclear magnetic resonance (NMR) spectroscopy has become a powerful tool for determining structure and functionality of biomolecular systems. Although there has been substantial progress in the development of efficient methods for deriving structural parameters from NMR experiments (see, e.g., refs 1−8), the assignment of experimental NMR spectra remains an important challenge.[9,10] Here, quantum chemical calculations of NMR chemical shifts can provide crucial information.

The quantum chemical calculation of NMR shieldings for molecules with more than 1000 atoms became accessible at the Hartree−Fock (HF) and density functional theory (DFT) levels, with recently developed linear- or even sublinear-scaling ab initio methods for these properties.[11−14] They not only allow for describing large molecules but also for systematically studying the convergence with respect to the necessary quantum chemical (QM) sphere (see, e.g., refs 15−18) if combined with simpler molecular mechanical (MM) approximations in so-called QM/MM schemes. In contrast, higher level wave function-based quantum chemical methods such as Møller−Plesset second-order perturbation theory (MP2)[19,20] or coupled cluster (CC) methods[21−23] are still limited to rather small molecules, although they would be highly desirable for calculating NMR shieldings in combination with sufficiently large basis sets.[18,24−31] While in recent years attempts have been made to improve efficiency at the MP2 level,[32−34] 1000 atoms cannot yet be described by such methods. Nevertheless, the simpler HF[35−40] or DFT[41−46] approaches often provide useful accuracies for NMR shieldings at this scale, and we will show the applicability of such methods here.

In the present work, we provide a systematic study on the convergence of NMR shieldings for a prototypical biochemical system for which we chose kaliotoxin,[47] *KTX*, a 38-residue peptide with 573 atoms. With our linear-scaling methods, we are able to abandon the often used approach to use di- or tripeptides as building blocks in NMR chemical shift predictions[48−53] and instead carry out a full expansion in the number of residues needed for a proper description of the chemical shifts. Furthermore, we do not utilize so-called locally dense basis sets[54] but describe all of the residues with the same basis set. The chemical shifts are first calculated with HF, DFT, and MP2 methods for small model systems within the gauge-including atomic orbitals (GIAO) ansatz to establish a valid method for approaching the full peptide system. In addition to the standard procedure for computing shieldings, we also employ an intermediate reference approach for calculating NMR chemical shifts in large molecules that provides an enhanced accuracy of the calculated shift values. This procedure has shown to be highly useful for predicting chemical shifts, e.g., in molecular tweezers.[55−57]

Received: August 9, 2013
Published: December 17, 2013

Also, empirical chemical shift prediction programs have been used to create chemical shifts based on the snapshots obtained from long molecular dynamics (MD) trajectories[58] and for intrinsically disordered proteins.[59−61] Predicted chemical shifts have also been used as restraints (pseudoforces) in the steered MD approaches.[62,63] However, the obvious drawback of empirical methods is the lack of systematic improvability that is offered in ab initio methods approximating the exact description of the Schrödinger equation. Thus, chemical shift values might be unrealistic due to the physical limitations in the empirical programs. For the same reason, the accuracy of the applied methods should be considered carefully when NMR relaxation data is obtained empirically through such programs[64] for correlated MD snapshots. While the empirical approaches offer the advantage of being much faster than quantum chemical calculations, their accuracy and sensitivity to structural changes is not clear.[65,66]

In our present work, we focus on a systematic study of six empirical chemical shift prediction programs (CAMSHIFT,[67] PROSHIFT,[68] SHIFTS,[69,70] SHIFTX,[71] SHIFTX2,[72] and SPARTA+[73]) in comparison to quantum chemical calculations. Here, we study the environmental and conformational sensitivity of NMR chemical shifts for the examples of both the *KTX* peptide comprising 573 atoms and an eight amino acid sequence. After a summary of computational details, we discuss first the methodological aspects for calculating NMR shieldings for large peptides and proteins. The effects of both basis sets and methods are studied. Also, the usefulness of the intermediate reference method is illustrated. The ab initio results are compared to empirical methods for calculating NMR shieldings, where in particular their sensitivity to the environment and conformational changes is discussed. Finally, the influence of solvent effects on the ab initio data is studied by systematic sampling over MD simulation snapshots.

2. COMPUTATIONAL DETAILS

Throughout this work, GIAOs[35,40,74] have been used in the ab initio computation of NMR shieldings. All GIAO-HF[40,75] shielding calculations were performed using linear-scaling techniques[11,12] and a density matrix-based Laplace reformulation of the coupled self-consistent field (DL-CPSCF) equations,[13,14] as implemented in a development version of the Q-Chem[76] program package. For GIAO-HF and GIAO-DFT shielding calculations, 6-31G**[77,78] as well as SVP, TZP, and QZ2P basis sets[79] were employed. Also def2-SVP and def2-TZVP basis sets[80] were used in the HF/DFT NMR shielding calculations. Corresponding GIAO-MP2[19,20,81] calculations with SVP, TZP, and QZ2P basis sets were carried out using the TURBOMOLE[82] program package. Selected GIAO-DFT calculations of NMR shieldings were performed with B3LYP,[83] B97-2,[84] and KT2[85] functionals. The nuclear shieldings were referred to NH_4^+ for nitrogen atoms and to tetramethylsilane (TMS) for carbon and hydrogen atoms to obtain the respective NMR chemical shifts. The structures of the reference molecules were optimized using TURBOMOLE at the MP2 level of theory including the resolution of identity approximation (RI-MP2)[86,87] with the TZVP basis set.

To describe the solvent effects in the context of conformational sensitivity of the ab initio NMR chemical shifts, MD simulations were carried out with the NAMD program package[88] using the *ff10* Amber force field.[89−91] The model amino acid sequence, Gln-Cys-Leu-Lys-Pro-Cys-Lys-Asp, is taken from the middle part of *KTX* and created as well as processed in the LEaP program.[92] For representative HF and DFT calculations in the vacuum, the sequence was saturated with hydrogens using the Avogadro program.[93] The solvent environment was introduced using the TIP3P water model[94] with LEaP. A total of 5663 water molecules were introduced in the simulation box. Initial runs involving heating at 600 K were used to provide a random starting point for the MD, and equilibration runs with both *NVT* (300 K) and *NPT* (300 K, 1 atm) ensembles were followed by a series of *NVE* production runs with a total length of roughly 20 ns. The *xyz* dimensions of the simulation box containing an eight residue amino acid sequence were {58.0, 57.6, 49.9 Å}, with a density of 1.02366 g/cm^3. Langevin thermostats[95] and barostats[96,97] were used. A time step of 1 fs, as well as periodic boundary conditions were used in all MD simulations.

Two structural snapshots were chosen from the final *NVE* MD trajectory with a time interval of 40 ps to avoid structural correlation. On the basis of these two structures, the final production *NVE* trajectories using the same water model were carried out with fixed atomic positions of the amino acids, so as to obtain the pure solvent effect for the NMR chemical shifts. The Cartesian coordinates of the two fixed conformers are deposited as Supporting Information (SI) (see Tables 1 and 2). From 10 to 1280 snapshots were obtained from both production MD *NVE* runs with a time interval of 6 ps between the snapshots and a radius of 6 Å around the amino acid sequence, corresponding to an average amount of 176 water molecules in the snapshot NMR calculations. The different sets of snapshots were collected with a 10 ps time interval between the individual sets so as to further avoid structural correlation. For these snapshot structures, ab initio shielding calculations were carried out with the Q-CHEM[76] program package at HF and DFT levels of theory. Ramachandran plots within the MolProbity program[98,99] did not show any torsion angle outliers[100] for the two peptidic conformations.

The empirically predicted chemical shifts from CAMSHIFT, PROSHIFT, SHIFTS, SHIFTX, SHIFTX2, and SPARTA+ (refs 67−73) program packages were compared against the ab initio data and experimental findings. SHIFTS calculates the NMR chemical shifts based on a density functional theory (DFT) database, while SHIFTX and its successor, the SHIFTX2 program, predict the NMR shifts using a hybrid approach combining classical equations and empirical chemical shift parametrized equations. Both PROSHIFT and SPARTA+ employ trained artificial neural networks to predict the NMR chemical shift values, whereas CAMSHIFT evaluates the chemical shifts based on polynomial functions of interatomic distances. For a detailed discussion on the methods, see refs 67−73.

3. METHODOLOGICAL ASPECTS

3.1. Influence of Basis Set and Method on NMR Chemical Shifts. The effects of the employed quantum chemical method and basis set on the NMR chemical shift values were explored using two different conformations of L-alaninaldehyde (for coordinates, see SI, Tables 4 and 5; for figures, see SI, Figure 1). Here, HF, B3LYP,[83,101−103] and BP86(VWN)[101,104−106] methods using a variety of basis sets are compared to MP2/QZ2P data as a reference (always using GIAOs). Overall, the typical behavior of accuracies is observed for NMR chemical shifts (see, e.g., refs 25−29 and 31); the corresponding data is only shown in the SI in Figure 2 and Tables 8−10.

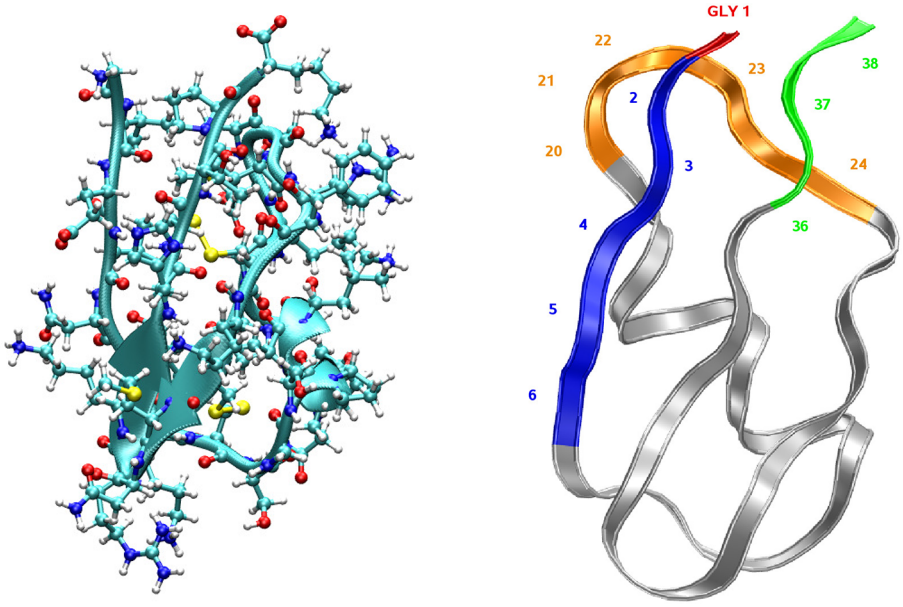

Figure 1. Left: NMR refined structure of kaliotoxin. Right: schematic sketch of kaliotoxin showing the neigboring residues for the calculation of N-terminal glycine chemical shifts.

Because the focus in our present work is on computing only differences between NMR chemical shifts (e.g., upon increasing the system size or between different conformations), it has to be stressed that error bars are systematically reduced as the electronic structures remain typically very similar. In this way, for example, for the two L-alaninaldehyde conformations, the maximum error at the HF/SVP level for nitrogen reduces from 12 to 3 ppm for shift differences (as compared to the most accurate MP2/QZ2P results). Similarly, the maximum HF/SVP deviations for carbon/hydrogen shifts decrease from 13 ppm/0.6 ppm to 2 ppm/0.3 ppm (the same holds for HF/6-31G**). For the same system, the maximum deviation for NMR shift differences of MP2/TZP as compared to MP2/QZ2P reduces to 0.6 ppm for nitrogen and carbon and to 0.2 ppm for hydrogen. For detailed data, see SI, Figure 3.

3.2. Intermediate Reference Method. An alternative route to improve the quality of NMR shift calculations is the use of an intermediate reference as outlined in the following. Because the calculation of MP2 shifts for large molecules with 500−1000 atoms is not feasible at the moment, a combination of the strengths of MP2 and HF NMR shift calculations would be desirable. Hence, a small fragment of the total molecular structure is chosen as the so-called intermediate reference system whose size is moderate enough to allow for the calculation of chemical shift values at the MP2 level. Then, in a second step, the influences of the environment (or also of the solvent) onto this fragment are accounted for at a lower level of theory (HF or DFT with often even smaller basis set is sufficient). This is justified because the description of such contributions only requires the calculation of shift differences that are much easier to describe because the electronic structure is less different. By this piecewise scheme of combining MP2 calculations for small fragments and HF calculations for the entire system, the both reliable and efficient calculation of chemical shifts becomes possible also for large molecular systems. Equationwise, the chemical shift of atom K is now expressed as

$$\delta_K^{\mathrm{MP2}} = \sigma_{\mathrm{Ref.}}^{\mathrm{MP2}} - \sigma_K^{\mathrm{MP2}} = (\sigma_{\mathrm{Ref.}}^{\mathrm{MP2}} - \sigma_{K,\mathrm{IR}}^{\mathrm{MP2}}) + (\sigma_{K,\mathrm{IR}}^{\mathrm{MP2}} - \sigma_K^{\mathrm{MP2}}) \quad (1)$$

$$\approx (\sigma_{\mathrm{Ref.}}^{\mathrm{MP2}} - \sigma_{K,\mathrm{IR}}^{\mathrm{MP2}}) + (\sigma_{K,\mathrm{IR}}^{\mathrm{HF}} - \sigma_K^{\mathrm{HF}}) \quad (2)$$

$$= \sigma_{\mathrm{Ref.}}^{\mathrm{MP2}} - (\sigma_{K,\mathrm{IR}}^{\mathrm{MP2}} + \sigma_K^{\mathrm{HF}} - \sigma_{K,\mathrm{IR}}^{\mathrm{HF}}) = \delta_K^{\mathrm{HF/MP2}} \quad (3)$$

where δ, σ, IR, and Ref. denote chemical shift, absolute shielding, intermediate reference, and standard reference, respectively.

In the following sections, the applicability of this so-called intermediate reference method (IRM) is evaluated using kaliotoxin (*KTX*) as a model system. Here, mainly three factors are influential and have to be taken into account when computing the chemical shifts of the amino acids in a protein or peptide: (1) molecular environment, (2) conformation of the involved amino acids, and (3) surrounding solvent of the amino acid sequence.

4. KALIOTOXIN AS A MODEL PEPTIDE

As a model system, we employed the 38-residue peptide kaliotoxin (*KTX*, see left-hand side of Figure 1) with the following sequence: Gly-Val-Glu-Ile-Asn-Val-Lys-Cys-Ser-Gly-Ser-Pro-Gln-Cys-Leu-Lys-Pro-Cys-Lys-Asp-Ala-Gly-Met-Arg-Phe-Gly-Lys-Cys-Met-Asn-Arg-Lys-Cys-His-Cys-Thr-Pro-Lys. The coordinates for the peptide were determined by an NMR-based structure optimization (see ref 47 for more details and also ref 107 for a more recent structure of the same peptide). From the NMR structure ensemble, the structure with the lowest RMSD value (denoted ktx2 in the following) was selected and used for the computational studies without further optimization. In the following, we examine the environmental, conformational, and solvent effects on the NMR chemical shifts for the N-terminal residue Gly1.

4.1. Environmental Influence on Gly1 Shifts. Using the program package Spartan, various subsystems of ktx2 were generated containing different amino acids of the peptide. Starting from fragment 1 (which includes only Gly1), further

dx.doi.org/10.1021/ct400713t | J. Chem. Theory Comput. 2014, 10, 122−133

Table 1. Chemical Shift Values of Glyl (first N-terminal residue in *KTX* saturated as zwitterion) by Systematically Enlarging the Calculated Fragment to the Full Sequence with 573 Atoms (shift denoted as δ_{KTX})[a]

	HF/SVP				MP2/TZP			
fragment	N	CA	C(O)	HA	N	CA	C(O)	HA
δ_{1}	14.3	43.1	187.5	3.4	19.9	48.7	171.9	3.5
$\delta_{1.2}$	12.2	41.6	167.2	2.8	17.9	46.8	154.9	2.9
$\delta_{1.2.3}$	11.6	41.1	169.2	2.9				
$\delta_{1.2.3.4}$	11.4	40.9	169.7	2.9				
$\delta_{1.2.3.4.5}$	11.4	40.9	170.0	2.9				
$\delta_{1.2.3.4.5.6}$	11.4	40.8	170.1	2.9				
$\delta_{1.3}$	14.1	43.0	186.8	3.4	19.6	48.7	172.2	3.5
$\delta_{1.4}$	14.3	43.1	187.5	3.4	19.9	48.7	172.0	3.5
$\delta_{1.21}$	14.4	43.1	187.5	3.4				
$\delta_{1.23}$	14.3	43.1	187.4	3.4	19.9	48.8	172.1	3.5
$\delta_{1.21.23}$	14.3	43.1	187.4	3.4				
$\delta_{1.21.22.23}$	14.3	43.1	187.4	3.4				
$\delta_{1.20.21.22.23.24}$	14.4	43.2	187.3	3.4				
$\delta_{1.37}$	13.9	42.3	187.0	3.7	19.6	47.5	172.3	3.7
$\delta_{1.36.37.38}$	13.9	42.3	187.3	3.8				
$\delta_{1.2.21.23.37}$	11.7	40.9	167.9	3.4				
$\delta_{1.2.3.21.23.37}$	11.2	40.4	169.7	3.4				
δ_{KTX}	11.0	40.3	171.1	3.4				

[a]Results in ppm, referenced to TMS and NH_4^+.

Table 2. Chemical Shift Values of Gly1.nh2 (first N-terminal residue in *KTX* saturated as amide structure) by Systematically Enlarging the Calculated Fragment to the Full Sequence[a]

	HF/SVP				MP2/TZP			
fragment	N	CA	C(O)	HA	N	CA	C(O)	HA
δ_{1}	11.1	39.8	172.7	2.9	16.5	44.6	162.1	3.0
$\delta_{1.2}$	11.2	40.8	170.4	3.0	17.0	46.2	159.0	2.9
$\delta_{1.2.3}$	11.3	40.9	169.6	2.9				
$\delta_{1.2.3.4}$	11.3	40.9	169.6	2.9				
$\delta_{1.4}$	11.2	39.8	172.5	2.9	16.6	44.6	161.8	3.0
$\delta_{1.23}$	11.1	39.7	172.6	2.9	16.6	44.5	161.9	3.0
$\delta_{1.37}$	10.8	39.4	172.6	3.3	16.3	44.1	162.1	3.4
$\delta_{1.2.3.23.37}$	10.9	40.3	169.9	3.3				
δ_{KTX}	11.0	40.3	171.1	3.4				

[a]Results in ppm, referenced to TMS and NH_4^+.

surrounding residues were added. In the same manner, for example, fragment 1.21.37 would include residues 1, 21, and 37. Tables 1 and 2 show the chemical shift values of these subsystems, whereas the subscripted numbers indicate the peptide residues included in the respective fragments. In addition, the chemical shifts for the entire *KTX* peptide with 573 atoms are given (labeled by δ_{KTX}). The closest residues, with their respective residue numbers, to Gly1 are shown on the right in Figure 1. Two saturation modes were used for the respective subsystems. For the zwitterionic case, Gly1 (and likewise the covalently connected residues) was saturated with an N-terminal ammonium ($-NH_3^+$) and a C-terminal carboxyl group ($-COO^-$), and all remaining residues were capped with neutral groups ($-NH_2$ and $-COOH$). As a second saturation variant, all C-termini were functionalized as amides, while the N-termini of further included fragments were saturated with aldehyde groups ($-NHCOH$). Solely, the N-terminus of Gly1 was still saturated with $-NH_3^+$ to obtain comparable shift values for the terminal nitrogen atom. One should bear in mind that Gly1 is not the only terminal residue for all peptide fragments considered here, so that the saturation, in a few cases, also affects other residues than Gly1.

In Tables 1 and 2, the chemical shift values for Gly1 are summarized for both saturation modes employing various subsystems at HF/SVP and MP2/TZP levels of theory. A comparison of NMR chemical shifts of fragment 1 to those of larger subsystems reveals a strong dependence of the environmental influence on the applied saturation mode. A similar behavior was observed in ref 108 where the effect of N-terminal charges on NMR chemical shifts of a peptide was investigated.

The NMR shifts of zwitterionic structures are strongly affected by the addition of neighboring amino acids (Table 1). The shift values of Gly1 at the HF level change up to 20 ppm for carbon and 0.6 ppm for hydrogen shifts when enlarging the calculated molecular size from fragment 1 to fragment 1.2. At the MP2 level, a similar behavior is observed with maximum changes of 17 ppm and 0.6 ppm, respectively. The impact of further neighboring amino acids decays rapidly. Equally, through-space interactions only moderately influence the NMR shifts of Gly1, as seen from the inclusion of residues further away from Gly1. At the HF level of theory, a maximum impact of a single noncovalently bound residue (number 37) is observed with the NMR shifts of Gly1 varying by 0.8 ppm for

dx.doi.org/10.1021/ct400713t | J. Chem. Theory Comput. 2014, 10, 122−133

Table 3. Chemical Shift Values (referred to TMS and NH_4^+) of Glycine in the *KTX* Conformation (GLY1), as well as in α-Helical and β-Sheet Conformations, Saturated as Amide Structures

		δ_{conf}			$\Delta_{\delta_{conf1}-\delta_{conf2}}$		
method	atom	δ_1	δ_α	δ_β	$\Delta_{\delta_\alpha-\delta_1}$	$\Delta_{\delta_\beta-\delta_1}$	$\Delta_{\delta_\alpha-\delta_\beta}$
HF/SVP	N	11.1	8.5	6.3	−2.6	−4.8	2.2
	CA	39.8	42.6	41.5	2.8	1.7	1.1
	C(O)	172.7	175.3	181.6	2.6	8.9	−6.3
	HA	2.9	4.2	4.2	1.3	1.3	−0.0
MP2/TZP	N	16.5	16.4	11.7	−0.1	−4.9	4.7
	CA	44.6	49.1	45.8	4.5	1.2	3.3
	C(O)	162.1	161.5	167.6	−0.6	5.5	−6.1
	HA	3.0	4.2	4.1	1.2	1.1	0.1

carbon/nitrogen and 0.3 ppm for hydrogen atoms comparing fragments 1 and 1.37. The MP2 shifts show similar trends. Fragment 1.2.3.21.23.37 captures nearly the entire impact of the peptide on Gly1 with remaining maximum errors (referred to the full peptide) of 1.4 ppm for carbon/nitrogen and less than 0.1 ppm for hydrogen shifts.

The saturation of the C-termini as amides leads to a decreased sensitivity of the calculated chemical shifts on inclusion of neighboring amino acids (Table 2). In contrast to the zwitterionic structures, the carbon and hydrogen shifts of Gly1 change only up to 2 ppm and 0.1 ppm at the HF/SVP and 3 ppm and 0.2 ppm at the MP2/TZP level, respectively, by adding the residue 2. Through-space interactions affect the Gly1 shifts in a very similar manner as described for the zwitterionic structures. This leads to a very good agreement between fragment 1 and the values for the entire peptide *KTX*, indicating that an amide saturation of the Gly1 C-terminus comprises most of the relevant influences on the Gly1 chemical shifts. Hence, the NMR shifts of Gly1 in subsystem 1.2.3.23.37 agree very well with the full *KTX* data within a range of 1 and 0.1 ppm for carbon and hydrogen shifts, respectively. Again, the environmental influence on Gly1 NMR shifts as studied in vacuo is very similar at the HF/SVP and MP2/TZP levels. In summary, maximum deviations between the shift differences between δ_1 and more complete peptidic representations of the two methods are 3 and 0.4 ppm (for ^{13}C and ^{1}H) in the zwitterionic structures and 1 ppm/0.1 ppm ($^{13}C/^{1}H$) using an amide saturation mode.

A comparison of the Gly1 shifts calculated for the subsystems to the values obtained for the complete peptide *KTX* consisting of 573 atoms affirms that the inclusion of the first covalently bound neighboring amino acid already contributes a main part of the environmental influence. However, for a sufficiently converged description, a cutoff radius of roughly 10 Å (roughly the three nearest amino acids in the sequence) within the almost linear peptide chain is needed for a reliable description of the Gly1 shifts in ktx2, in line with previous studies on other systems.[18] However, it should be mentioned that Gly1 is positioned at the outer surface of ktx2. Thus, residues more deeply buried within the peptide, or close to the active site of a protein, may require even a larger environment for a proper description of the respective chemical shifts (see, e.g., ref 18).

4.2. Conformational Influence on Gly1 Shifts. To examine the conformational influence on the Gly1 NMR chemical shifts, two additional conformers of glycine in α-helical and β-sheet arrangement were generated using the Spartan program. These conformers were created as if they were part of a chain of glycine residues either in α-helix or in a β-sheet. No further structural optimizations were carried out for the glycine in the desired conformation. An amide saturation was chosen for all three conformers (for coordinates, see SI, Tables 3, 6, and 7).

In Table 3, the NMR chemical shifts of the conformers (δ) and the shift differences between the conformations (Δ_δ) are summarized. The conformational influence on the HF/SVP chemical shifts, (Δ_δ), is up to 9 ppm for ^{13}C and 1.3 ppm for ^{1}H, which is in line with other studies on conformational effects in NMR shift calculations.[109−111] Comparable results are found with the MP2/TZP method, where shift changes between the conformers of up to 6 ppm/1.2 ppm ($^{13}C/^{1}H$) occur. As in the case of the observed environmental influence, the HF/SVP and the MP2/TZP shift differences emerging from conformational changes agree quite well within a range of 3 ppm for ^{13}C and 0.3 ppm for ^{1}H shifts. Thus, the use of the HF method for describing the conformational and environmental effects on NMR chemical shifts appears as a good compromise for the molecules studied, which in turn strengthens the applicability of the aforementioned intermediate reference method for NMR shift calculations on peptidic systems.

4.3. Empirical Methods for Calculating NMR Chemical Shifts. Besides ab initio methods, a variety of empirical approaches are available for calculating chemical shifts of biomolecular systems. Such approaches are often used in structure determination processes[112] and for the recalculation of chemical shifts in order to approve and validate derived structure models.[113] In contrast to ab initio calculations, empirical approaches are extremely fast in computing chemical shifts due to their parametrized functional form. The drawback is of course that such schemes do not account for the electronic structure explicitly, so that the sensitivity to changes in the electronic structure caused, for example, by environmental, conformational, or solvent effects needs to be checked carefully, which is the focus of our present work.

In the following, ab initio NMR chemical shifts are compared to results obtained using six empirical prediction programs: CAMSHIFT, PROSHIFT, SHIFTS, SHIFTX, SHIFTX2, and SPARTA+. In order to compare them, we reference the data obtained to the experimental values. It has to be stressed that a comparison of our ab initio data described above to the experiment is quite meaningless in itself because these calculations have been performed in the vacuum and the experimental results emerge from the solid state. A full account of the crystal structure (or in solution, water, or any other solvent environment) for the KTX NMR spectrum at the ab initio level is beyond the scope of our present study because we aim instead to compare the sensitivity of empirical calculation

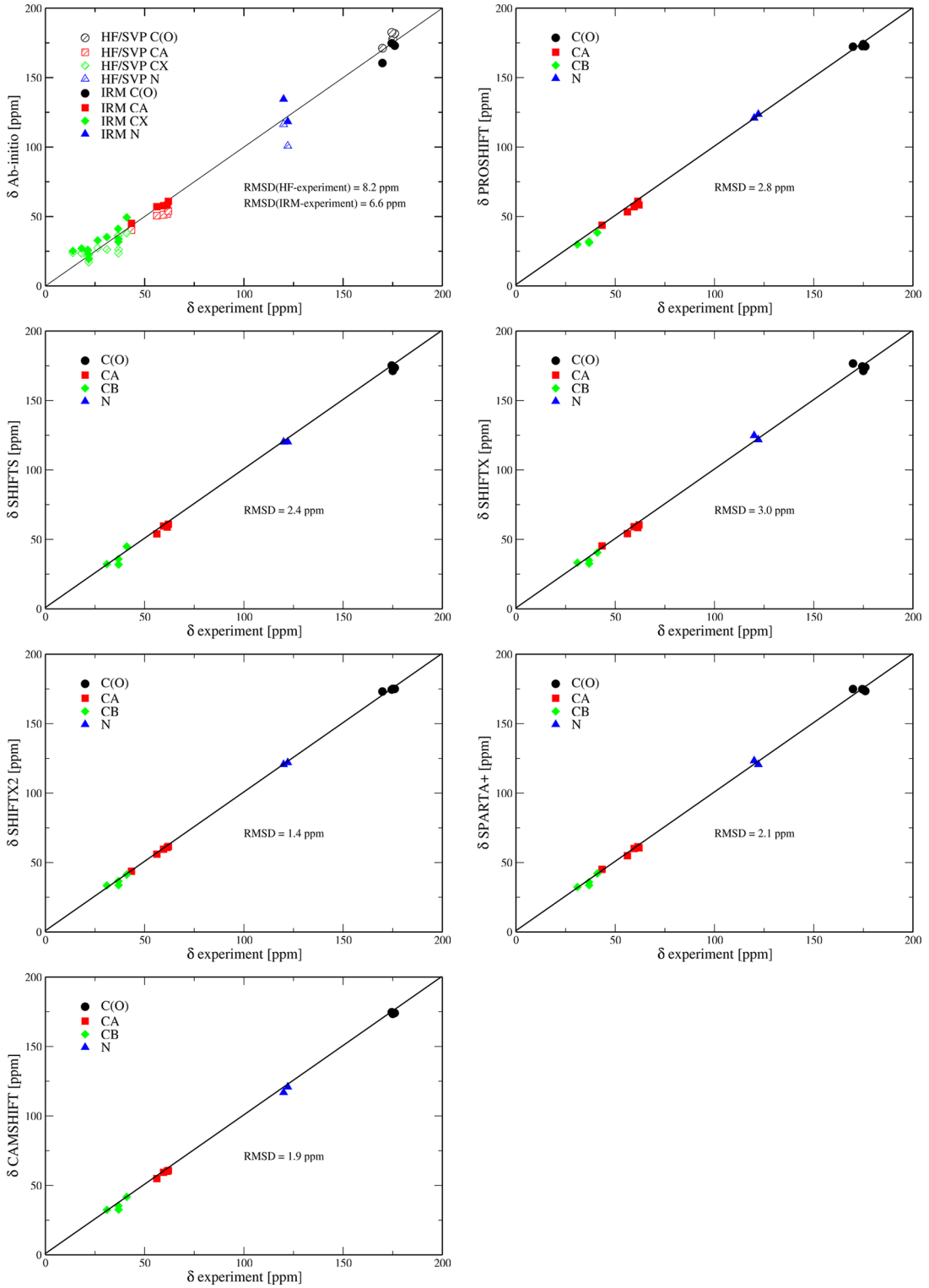

Figure 2. Experimental[114] and calculated NMR chemical shifts for structure model ktx2 of *KTX* (results shown only for the first six residues). IRM stands for intermediate reference method. See text for details.

models. Although there are a variety of continuum models available in the literature, many influences are difficult to describe using simple continuum models and an explicit account of solvent effects using MD simulations would require extensive and costly sampling at the ab initio level over many water conformations. Thus, we focus here on comparing the sensitivity of ab initio and empirical models upon changes due to the environment (either molecular or solvent) and to conformations. For the smaller peptidic model systems, we also studied the influences of an explicit solvent and the convergence with the number of snapshots chosen for statistical averaging.

The differences between the various schemes for the full KTX system are nicely illustrated in the correlation diagrams

dx.doi.org/10.1021/ct400713t | *J. Chem. Theory Comput.* 2014, 10, 122−133

Table 4. Environmental Influence Δ_{Val2} on Chemical Shift Values δ_{Val2} of Second Residue in *KTX* (valine)

		influence on second residue of *KTX* by enlarging calc. fragment			
	atom	HF/SVP	PROSHIFT	SHIFTS	SHIFTX
$\Delta_{Val2}(1.2.3-1.2.3.4)^a$	N	2.5		−1.6	0.0
	CA	0.1	—[b]	0.0	0.0
	C(O)	−1.8		2.7	0.7
	CB	0.3		0.1	0.1
$\Delta_{Val2}(1.2.3-1.2.3.4.5.6)^a$	N	4.2		−1.6	0.0
	CA	0.1	—[b]	0.0	0.0
	C(O)	−2.5		2.7	0.7
	CB	0.5		0.1	0.1
$\Delta_{Val2}(1.2.3-ktx2)^a$	N	11.1		−1.6	0.0
	CA	0.7	—[b]	0.0	0.0
	C	−5.3		2.7	0.7
	CB	0.9		0.1	0.1

[a] $\Delta_{Val2}(\text{Fragment1} - \text{Fragment2}) = \delta_{val2}(\text{Fragment1}) - \delta_{val2}(\text{Fragment2})$. [b] For the first two amino acids of the peptide chain, only averaged database values are available, so no influence can be determined.

shown in Figure 2 comparing both vacuum ab initio and empirical results with experimental NMR chemical shifts. For the calculations, the entire structure (ktx2) was employed using the HF/SVP method and the empirical approximations denoted above. In addition, the intermediate reference procedure combining MP2/TZP and HF/SVP was used for residues 1 to 6, thus only the values for these residues are shown. As the experimental solid-state NMR data provided by the group of Prof. Marc Baldus is restricted only to carbons and nitrogens,[47,114] we discuss only these atom types. Naturally, some of the errors between the experimental solid-state and computed NMR chemical shifts arise from the fact that computations are carried out in vacuum, as opposed to experiments performed in the solid state.

The correlation diagrams (Figure 2) reveal a rather good agreement—within the root-mean-square deviation (RMSD) range of 1.4 to 3.0 ppm—between experimentally derived shifts and results of the empirical calculations. This may be explained by the way empirical approaches are commonly designed based on parameters derived from bulk observed properties or from large data sets produced by less demanding quantum chemical calculations, which both are fundamentally statistical. Similarly, experimental values are also statistical averages over all possible conformations present in the sample.

As expected and discussed above, the vacuum ab initio results show large deviations from the experimental values. The same holds, to a smaller degree, if an intermediate reference system is employed that is expected to improve the reliability of the results. While the ab initio shifts of the backbone carbons CA and C(O) agree better with experimental values, this is less so for the amino acid side chains that are more exposed to the missing environment in the vacuum calculation.

4.4. Influence of Environment at ab Initio and Empirical Level of Theory. While the empirical approaches agree with the experimental NMR data of the *KTX* peptide within a maximum RMSD value of 3.0 ppm, we study here their sensitivity in accounting for structural changes and focus first on the environment.

In Table 4, the influences of different environments on the NMR shifts of residue Val2 in ktx2 are summarized. As the smallest subsystem, the tri-peptide 1.2.3 was chosen because some of the employed empirical approaches do not determine the NMR chemical shifts for the terminal residues. In addition, the database nature of SHIFTX and SHIFTS methods enforced to employ standard saturation modes and, thus, a zwitterionic saturation was used.

HF/SVP results show a considerable environmental influence on the Val2 shifts. The addition of residue 4 changes the Val2 NMR shifts up to 2 ppm for carbon and 3 ppm for nitrogen atoms. Furthermore, including residues 5 and 6 still has a non-negligible 1 ppm effect on Val2 ^{13}C and ^{15}N shifts. Particularly the inclusion of through-space interactions by calculating the complete peptide influences Val2 with maximum shift changes of 5 ppm (^{13}C) and 11 ppm (^{15}N). These observations are in line with expected influences of the electronic structure.

In contrast, the results for both the SHIFTS and SHIFTX program packages show much less sensitivity to the local environment and deviate up to more than 8 and 13 ppm, respectively, from the HF/SVP ab initio data. For SHIFTS, the Val2 shifts change by a maximum of 3 ppm (^{13}C) when adding residue 4, and no further changes occur comparing 1.2.3.4 to fragment 1.2.3.4.5.6 or the complete peptide *KTX*. This behavior can be understood as the underlying DFT database of the SHIFTS program considering only the direct and next-neighbor conformational effects, in addition to the hydrogen bonds through the space, which are not present for Val2 in ktx2. A similar reasoning holds for the SHIFTX package. Here, the environmental influence on the Val2 shifts is even smaller than seen for SHIFTS with a maximum shift change of 1 ppm (^{13}C) when including residue 4 in the calculation. The statistically derived hypersurfaces employed in SHIFTX are based on experimental NMR shifts and include only similar effects as the DFT database of SHIFTS. In addition, both programs do not account for local charge effects that should affect the NMR shift of Val2 by expanding the calculated fragment.

Because in the training set of the PROSHIFT package not only next neighbor effects but also through space interactions to atoms close in space are described, it is expected to be most sensitive to environmental effects within the empirical approaches. However, PROSHIFT does not explicitly determine the NMR shifts of the two respective terminal residues but attributes default database values instead, so that PROSHIFT is not suitable for the calculation of short sequences and was omitted in this section.

Overall, the three employed empirical approaches appear to be not suitable for a detailed description of environmental

Table 5. Differences of Chemical Shifts between the Two Structure Models ktxR and ktx2 to Denote Conformational Sensitivity

			method			
residue number	residue type	atom type	HF/SVP	PROSHIFT	SHIFTX	SHIFTS
1	GLY	C(O)	−0.3	0.0	−3.8	—
6	VAL	C(O)	−3.4	−0.3	0.2	0.3
2	VAL	CA	−2.4	0.0	2.0	1.8
3	GLU	CA	−4.6	0.0	0.3	0.3
4	ILE	CA	4.2	0.7	−0.2	−0.5
2	VAL	CB	5.1	0.0	1.5	2.1
4	ILE	CB	11.5	−0.2	−0.5	−0.6
5	ASN	CB	5.2	−0.2	1.3	0.2
5	ASN	CG	−7.2	0.3	—	—
3	GLU	N	12.7	−2.4	−1.7	2.2
5	ASN	N	−3.9	1.6	3.1	2.7
6	VAL	N	−2.1	−0.5	2.4	−8.7
8	CYS	N	13.5	−2.3	−2.0	—
10	GLY	N	−0.2	2.9	−2.8	−2.7

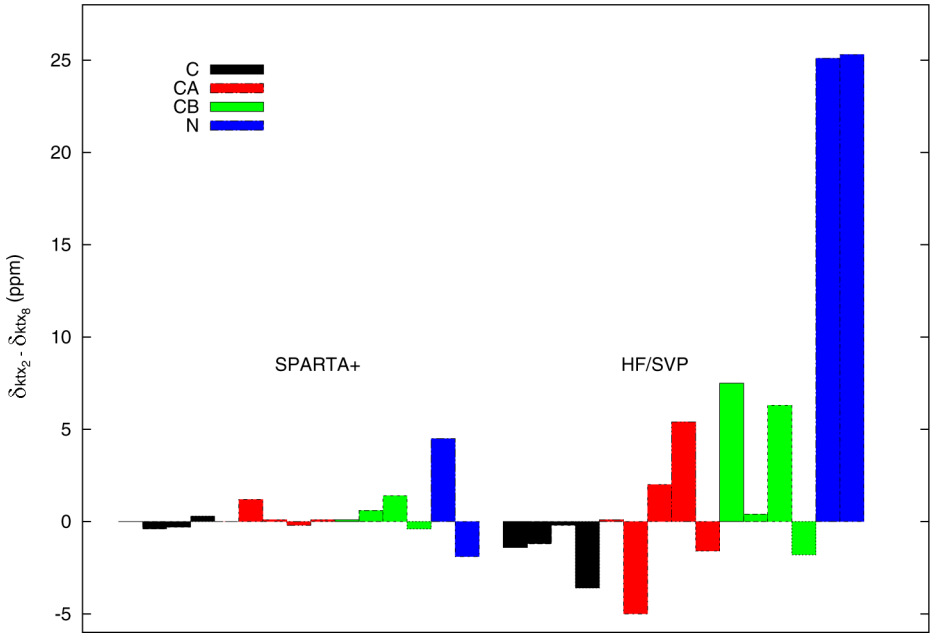

Figure 3. Empirical and computed NMR shift differences between structure models 2 and 8 taken from the NMR ensemble of *KTX*. Both SPARTA+ and HF/SVP methods are used to illustrate the conformational sensitivity. Only chemical shifts for nuclei in the first six residues are being considered here.

influences, either due to lacking information in their underlying databases (SHIFTS and SHIFTX) or caused by their restricted applicability on short sequences (PROSHIFT). It should be stressed that this stands in contrast to ab initio calculations, which mark an expected high sensitivity to environmental changes.

4.5. Conformational Influence at ab Initio and Empirical Level of Theory. As mentioned in the previous section, the empirical approximations are rather insensitive to environmental changes, so that we study in the following the sensitivity to conformational changes that involve an intricate interplay of electronic structure effects. As a representative example, we consider in the following the shift differences arising between two structures of the experimentally proposed NMR ensemble. Here, we chose structure model ktx2 and a randomly selected second structure from the NMR ensemble (denoted as ktxR) as shown in Table 5.

The two employed *KTX* structures yield strongly differing NMR spectra as computed at the HF/SVP level. The shifts of ktxR and ktx2 differ up to 12 ppm for carbon and 14 ppm for nitrogen in the ab initio calculations.

This observation contrasts the results of the empirical calculations with PROSHIFT and SHIFTX that show only influences of up to 3 or 4 ppm, respectively. Although SHIFTS yields changes of up to 9 ppm, the pattern of the shift differences between the two conformations is in all three empirical programs drastically different from the more reliable ab initio results (Table 5). This clearly shows the insensitivity of empirical calculations to both environmental and structural changes.

As a further example of conformational sensitivity, in Figure 3, we compare the NMR shift differences of structure models 2 and 8 taken from the NMR ensemble of *KTX*, calculated with both the SPARTA+ program and HF/SVP method. The HF/

dx.doi.org/10.1021/ct400713t | J. Chem. Theory Comput. 2014, 10, 122−133

Table 6. Representative Carbon and Nitrogen Shift Differences of Two Different Conformations of an Unsaturated Model Amino Acid Sequence (Gln-Cys-Leu-Lys-Pro-Cys-Lys-Asp) as a Function of the Number of Solvent Snapshots at HF/SVP Level of Theory

			number of snapshots[a]							
residue nr/type	atom type	vacuum	10	20	40	80	160	320	640	1280
2/CYS	C(O)	−9.2	−12.7	−11.2	−11.2	−11.0	−11.7	−11.0	−11.1	−11.2
3/LEU	C(O)	1.2	−0.4	0.1	−0.2	0.0	−0.7	−0.5	−0.3	−0.5
4/LYS	C(O)	−14.5	−15.3	−15.1	−14.3	−15.3	−15.8	−15.9	−15.9	−15.9
5/PRO	C(O)	5.9	4.2	2.9	4.2	3.9	4.2	3.8	3.9	3.7
6/CYS	C(O)	−15.0	−14.2	−16.2	−14.7	−14.5	−14.2	−14.3	−14.2	−14.4
7/LYS	C(O)	12.1	12.7	12.0	12.2	12.1	11.4	11.3	11.4	11.5
2/CYS	CA	−0.1	−0.3	−1.5	−0.9	−1.0	−2.7	−1.4	−1.5	−1.6
3/LEU	CA	−2.0	−2.2	−1.6	−1.7	−1.7	−1.9	−1.9	−1.9	−1.9
4/LYS	CA	−6.4	−5.3	−5.4	−5.6	−5.9	−5.9	−5.8	−5.9	−5.9
5/PRO	CA	−3.5	−4.9	−4.1	−3.8	−3.4	−3.7	−3.4	−3.5	−3.5
6/CYS	CA	1.4	1.4	1.4	1.6	1.9	1.6	1.7	1.5	1.6
7/LYS	CA	3.2	2.2	1.8	2.5	2.8	2.5	2.7	2.8	2.8
2/CYS	CB	−1.9	−0.8	−1.1	−1.0	−0.9	−0.8	−1.0	−0.9	−1.0
3/LEU	CB	−10.1	−8.6	−8.9	−8.5	−8.5	−9.8	−9.0	−8.9	−8.8
4/LYS	CB	3.7	4.6	4.5	4.7	4.0	4.1	4.1	4.2	4.2
5/PRO	CB	−2.5	−2.3	−2.3	−2.2	−2.4	−2.1	−2.3	−2.3	−2.2
6/CYS	CB	−2.1	−2.9	−2.4	−3.1	−2.9	−2.8	−3.3	−2.9	−3.1
7/LYS	CB	1.9	1.4	1.5	1.7	1.1	1.4	1.5	1.4	1.4
2/CYS	N	−5.8	−3.6	−2.9	−3.4	−4.7	−2.6	−3.9	−3.8	−3.9
3/LEU	N	−17.4	−17.2	−14.0	−14.2	−13.2	−16.5	−15.1	−15.9	−15.4
4/LYS	N	−3.8	−4.0	−3.1	−5.4	−4.6	−5.7	−4.5	−5.1	−5.0
5/PRO	N	−5.9	−10.6	−11.0	−7.1	−5.7	−7.3	−5.8	−7.6	−7.1
6/CYS	N	−8.2	−6.3	−5.1	−4.0	−5.6	−6.7	−6.2	−6.0	−6.1
7/LYS	N	−5.4	−10.0	−15.2	−11.6	−8.7	−8.4	−7.1	−7.3	−7.7
	RMSD[b]	1.3	1.1	1.1	0.7	0.7	0.5	0.3	0.2	

[a]QM values are averages over 10 to 1280 snapshots cut from the trajectory with a radius of 6 Å around the fixed amino acid conformations at time intervals of 6 ps apart. [b]Root-mean-square deviations (RMSD) of vacuum and solvent-including calculations with respect to the value obtained using 1280 snapshots.

SVP results depict a much higher overall sensitivity toward structural changes than the empirical SPARTA+ method.

4.6. Accuracies and Solvent Effects on Conformational Sensitivity. While the differences in sensitivity of ab initio vs empirical methods is most striking, the question may arise whether solvent effects or the choice of the quantum chemical method could damp out the conformational sensitivity found in the first-principles NMR chemical shifts. Therefore, we probe in the following the influences of different QM methods, basis sets, and the inclusion of explicit solvent effects, the latter also in dependence of the number of solvent snapshots.

The influence of different basis sets on the shielding differences for two different conformers of a model amino acid sequence of *KTX*, Gln-Cys-Leu-Lys-Pro-Cys-Lys-Asp, is probed both in vacuum and in explicit aqueous solvent. The carbon and nitrogen data show only a relatively small influence of basis sets with maximum changes of 1 and 2 ppm between SVP and def-TZVP basis sets both in vacuum and in solution, respectively (see data in SI, Table 12). Note that this comparably high accuracy is obtained already with the fairly small SVP basis sets for carbon or nitrogen, which is due to the consideration of only structural/conformational changes. While the results are not entirely converged in terms of basis set, we expect only minor influences remaining, so that the results fully support the observed strong changes of NMR shieldings between conformers.

In addition, we studied the influences of different ab initio methods on the conformational sensitivity of the NMR shielding differences. Apart from the common B3LYP functional, both B97-2 and KT2 functionals are tested based on their earlier good performance in producing NMR chemical shifts with respect to correlated ab initio methods.[18] In general, the different methods provide the same trends in all cases, with deviations of only up to 2 ppm in the shielding differences of carbon atoms between the different QM results (see data in SI, Table 13). While larger changes of up to roughly 6 ppm are observed for the nitrogen atoms, the strong sensitivity toward structural changes is maintained. In future work, we expect new and ongoing developments of linear- or sublinear-scaling MP2 methods for calculating NMR shieldings[34] to provide access to even more reliable results also for large molecules.

The conformational sensitivity observed at the quantum chemical level for NMR shielding differences remains also if explicit solvent is included (Table 6). Here, the differences were computed by dynamical averaging over up to 1280 molecule configurations as obtained from an MD trajectory (see Computational Details), while keeping the amino acid sequences fixed. Thus, only the positions of the water molecules, and not the conformations of the peptide chain itself, are changed as solvent effects are introduced. No results for the terminal residues are shown because there are several ways to saturate the sequences, and no detailed study on the dependence on the saturation scheme was performed here. In order to ensure convergence with the sampling space, we simulated the solvent NMR spectrum in water by systematically increasing the number of solvent configurations to up to 1280. The RMS deviation changes by roughly 0.2 ppm with the

Table 7. Quantum Mechanically Calculated and Semi-Empirically Predicted Representative Carbon and Nitrogen Shift Differences between Two Different Conformations of an Unsaturated Model Sequence of Eight Amino Acids (Gln-Cys-Leu-Lys-Pro-Cys-Lys-Asp)

		HF/SVP		prediction programs					
residue nr/type	atom type	vac.	sol.[a]	PROSHIFT	SHIFTS	SPARTA+	SHIFTX	SHIFTX2	CAMSHIFT
2/CYS	C(O)	−9.2	−11.2	0.0	0.0	0.8	0.5	0.4	−1.0
3/LEU	C(O)	1.2	−0.5	0.9	3.0	1.0	1.1	1.0	0.9
4/LYS	C(O)	−14.5	−15.9	0.2	−0.9	0.5	0.7	1.0	1.7
5/PRO	C(O)	5.9	3.7	−0.6	−0.4	0.6	0.2	0.1	0.5
6/CYS	C(O)	−15.0	−14.4	0.7	0.0	0.2	0.6	0.0	−0.1
7/LYS	C(O)	12.1	11.5	0.0	0.0	0.1	−0.2	−0.2	−0.4
2/CYS	CA	−0.1	−1.6	0.0	0.0	−1.2	−1.5	−1.6	−2.0
3/LEU	CA	−2.0	−1.9	−1.2	2.1	0.0	2.0	2.2	2.2
4/LYS	CA	−6.4	−5.9	0.9	2.3	1.1	1.7	1.5	1.1
5/PRO	CA	−3.5	−3.5	0.7	−0.9	0.1	0.3	0.4	−1.3
6/CYS	CA	1.4	1.6	−0.4	0.0	0.3	0.3	0.1	1.2
7/LYS	CA	3.2	2.8	0.0	0.4	0.5	0.7	1.0	1.4
2/CYS	CB	−1.9	−1.0	0.0	0.0	0.8	0.7	0.0	0.0
3/LEU	CB	−10.1	−8.8	−0.8	0.8	0.4	0.0	0.0	−0.6
4/LYS	CB	3.7	4.2	−1.0	−3.4	−2.4	−3.1	−1.7	−1.7
5/PRO	CB	−2.5	−2.2	0.4	−1.4	−0.2	0.0	0.0	0.1
6/CYS	CB	−2.1	−3.1	0.0	0.0	0.3	−3.4	0.2	−1.3
7/LYS	CB	1.9	1.4	0.0	−0.2	0.1	−0.2	0.1	0.3
2/CYS	N	−5.8	−3.9	0.0	0.0	1.4	3.3	4.9	0.6
3/LEU	N	−17.4	−15.4	−0.7	−7.0	−1.8	1.2	1.0	1.9
4/LYS	N	−3.8	−5.0	2.3	0.1	1.2	1.4	1.9	−0.6
5/PRO	N	−5.9	−7.1	0.1	4.3	0.0	0.0	0.0	0.0
6/CYS	N	−8.2	−6.1	−1.5	0.0	1.1	−0.5	−0.5	−2.4
7/LYS	N	−5.4	−7.7	0.0	−0.3	0.6	1.1	0.2	−1.7

[a]Solvated QM values are averages over 1280 snapshots each containing on the average 645 atoms cut out from the trajectory within a radius of 6 Å from the amino acid sequence at time intervals of 6 ps apart.

transition from 640 to 1280 snapshots, so that the results can be regarded to be sufficiently converged.

In Table 7, both vacuum and solvent-including QM results behave fairly similarly. In general, both alpha and beta carbons in different amino acids are less influenced by the solvent than C(O) and nitrogen nuclei. The RMSD between the values calculated in solvent and in vacuum is about 1.3 ppm, when the solvent-including shielding differences are obtained from 1280 snapshots. Overall, the solvent data show that the sensitivity to conformational changes remains high also in solution.

In Table 7, the ab initio results both in vacuum and within the water solvent (1280 snapshots) are compared to shift differences computed using the empirical chemical shift prediction programs CAMSHIFT, PROSHIFT, SHIFTS, SHIFTX, SHIFTX2, and SPARTA+. The data clearly confirm drastically different and insensitive behavior of the empirical schemes to structural changes. Neither the magnitude nor the pattern observed at the ab initio level is reproduced by the empirical programs. The lack of sensitivity in the studied empirical approaches for the present molecular systems makes their use in validating the predicted structures questionable.

5. CONCLUSIONS

We have presented a comparison of the sensitivity of ab initio versus empirical approaches in computing structural effects on NMR chemical shifts for the example of a peptide, kaliotoxin, comprising 573 atoms, as well as for a peptide fragment with eight amino acids. The results of empirical approaches (CAMSHIFT, PROSHIFT, SHIFTS, SHIFTX, SHIFTX2, and SPARTA+) clearly show the structural insensitivity for determining NMR chemical shifts, so that their use for checking the reliability of a predicted structure model has to be carefully studied. At the same time, it has to be noted, that they correlate fairly well with the experimental data in this representative case because the empirical methods are intrinsically statistical. In contrast, ab initio chemical shift data show a high sensitivity to structural changes. The accuracy of the employed quantum chemical approaches was investigated by using electron correlation methods and various basis sets. Here, the accuracy for describing NMR shielding differences is much higher than for absolute shieldings because the electronic structure is more similar. This favorable effect is also employed in the intermediate reference method. Furthermore, an explicit account of solvent effects has been studied using molecular dynamics simulations with up to 1280 sampling points confirming the convergence. All results support the validity of the strong structural influence on NMR chemical shifts observed by employing ab initio methods. This contrasts the behavior of the empirical approaches for specific molecular conformations that neither reproduce the magnitude nor the patterns of ab initio chemical shifts. While ab initio methods do not suffer from this insensitivity, the computational cost is clearly larger than for empirical methods. This is particularly true due to the required sampling over snapshots for describing solvent effects in an explicit fashion. Nevertheless, with newly developed and faster ab initio methods, larger systems are becoming accessible to reliable NMR shielding calculations at the quantum chemical level. This opens not only new possibilities for the ab initio assignment of experimental NMR data but also for providing better and more extensive

reference data for parametrizing empirical models, both of which have been and will continue to be valuable tools for interpreting NMR spectra.

■ ASSOCIATED CONTENT

Supporting Information

Tables containing the Cartesian coordinates of the peptidic conformers, as well as the conformers of L-alaninaldehyde (with figures also) and glycine; figures and tables containing nitrogen, carbon, and hydrogen chemical shifts and shift differences for α- and β-L-alaninaldehyde at various levels of theory; and tables containing the basis set and QM theory dependence of representative nitrogen and carbon chemical shifts for the eight-residue peptidic conformers. This material is available free of charge via the Internet at http://pubs.acs.org.

■ AUTHOR INFORMATION

Corresponding Author

*E-mail: christian.ochsenfeld@cup.uni-muenchen.de.

Present Address

‡Matti Hanni: Department of Radiology, University of Oulu, P. O. Box 5000, FIN-90014, University of Oulu, Oulu, Finland.

Notes

The authors declare no competing financial interest.

■ ACKNOWLEDGMENTS

The authors thank Dr. Denis Flaig, Dr. Jörg Kussmann, Dr. Boris Maryasin, and Simon Maurer (LMU Munich) for useful discussions. In addition, Prof. Dr. Marc Baldus (Utrecht University, The Netherlands) is thanked for kindly providing the coordinates of the kaliotoxin peptide. C.O. acknowledges financial support by the Volkswagen Stiftung within the funding initiative "New Conceptual Approaches to Modeling and Simulation of Complex Systems", by the SFB 749 "Dynamik und Intermediate molekularer Transformationen" (DFG), and the DFG cluster of excellence EXC 114 "Center for Integrative Protein Science Munich" (CIPSM).

■ REFERENCES

(1) Creuzet, F.; McDermott, A.; Gebhard, R.; van der Hoef, K.; Spijker-Assink, M.; Herzfeld, J.; Lugtenburg, J.; Levitt, M. H.; Griffin, R. G. *Science* **1991**, *251*, 783−786.

(2) Cross, T. A.; Opella, S. J. *Curr. Opin. Struct. Biol.* **1994**, *4*, 574−581.

(3) Griffin, R. G. *Nat. Struct. Biol.* **1998**, *5*, 508−512.

(4) Ando, I.; Kameda, T.; Asakawa, N.; Kuroki, S.; Kurosu, H. *J. Mol. Struct.* **1998**, *441*, 213−230.

(5) Wider, G. *BioTechniques* **2000**, *29*, 1278−1294.

(6) Rienstra, C. M.; Tucker-Kellogg, L.; Jaroniec, C. P.; Hohwy, M.; Reif, B.; McMahon, M. T.; Tidor, B.; Lozano-Pérez, T.; Griffin, R. G. *Proc. Natl. Acad. Sci. U.S.A.* **2002**, *99*, 10260−10265.

(7) Wüthrich, K. *Angew. Chem., Int. Ed.* **2003**, *42*, 3340−3363.

(8) Opella, S. J.; Marassi, F. M. *Chem. Rev.* **2004**, *104*, 3587−3606.

(9) Huang, C.; Mohanty, S. *J. Am. Chem. Soc.* **2010**, *132*, 3662−3663.

(10) Bellstedt, P.; Seiboth, T.; Häfner, S.; Kutscha, H.; Ramachandran, R.; Görlach, M. *J. Biomolec. NMR* **2013**, *57*, 65−72.

(11) Ochsenfeld, C.; Kussmann, J.; Koziol, F. *Angew. Chem., Int. Ed.* **2004**, *43*, 4485−4489.

(12) Kussmann, J.; Ochsenfeld, C. *J. Chem. Phys.* **2007**, *127*, 054103:1−16.

(13) Beer, M.; Ochsenfeld, C. *J. Chem. Phys.* **2008**, *128*, 221102:1−4.

(14) Beer, M.; Kussmann, J.; Ochsenfeld, C. *J. Chem. Phys.* **2011**, *134*, 074102:1−15.

(15) Senn, H. M.; Thiel, W. In *Atomistic Approaches in Modern Biology*; Reiher, M., Ed.; Topics in Current Chemistry Series; Springer: Berlin Heidelberg, 2007; pp 173−290.

(16) Sumowski, C. V.; Ochsenfeld, C. J. *Phys. Chem. A* **2009**, *113*, 11734−11741.

(17) Meier, K.; Thiel, W.; van Gunsteren, W. F. *J. Comput. Chem.* **2012**, *33*, 363−378.

(18) Flaig, D.; Beer, M.; Ochsenfeld, C. *J. Chem. Theory Comp.* **2012**, *8*, 2260−2271.

(19) Gauss, J. *Chem. Phys. Lett.* **1992**, *191*, 614−620.

(20) Gauss, J. *J. Chem. Phys.* **1993**, *99*, 3629−3643.

(21) Gauss, J.; Stanton, J. F. *J. Chem. Phys.* **1995**, *102*, 251−253.

(22) Gauss, J.; Stanton, J. F. *J. Chem. Phys.* **1995**, *103*, 3561−3577.

(23) Gauss, J.; Stanton, J. F. *J. Chem. Phys.* **1996**, *104*, 2574−2583.

(24) Gauss, J. Molecular Properties. In *Modern Methods and Algorithms of Quantum Chemistry*; Grotendorst, J., Ed.; Winterschool: Jülich, Germany, **2000**; p 541.

(25) Jensen, F. *J. Chem. Theory Comp.* **2008**, *4*, 719−727.

(26) Auer, A. A.; Gauss, J.; Stanton, J. F. *J. Chem. Phys.* **2003**, *118*, 10407−10417.

(27) Cheeseman, J. R.; Trucks, G. W.; Keith, T. A.; Frisch, M. J. *J. Chem. Phys.* **1996**, *104*, 5497−5509.

(28) Zuschneid, T.; Fischer, H.; Handel, T.; Albert, K.; Häfelinger, G. *Z. Naturforsch.* **2004**, *59b*, 1153−1176.

(29) Helgaker, T.; Jaszuński, M.; Ruud, K. *Chem. Rev.* **1999**, *99*, 293−352.

(30) Teale, A. M.; Lutnæs, O. B.; Helgaker, T.; Tozer, D. J.; Gauss, J. *J. Chem. Phys.* **2013**, *138*, 024111:1−21.

(31) Flaig, D.; Maurer, M.; Hanni, M.; Braunger, K.; Kick, L.; Thubauville, M.; Ochsenfeld, C. submitted for publication to *J. Chem. Theory Comp.* (2013).

(32) Gauss, J.; Werner, H.-J. *Phys. Chem. Chem. Phys.* **2000**, *2*, 2083−2090.

(33) Loibl, S.; Schütz, M. *J. Chem. Phys.* **2012**, *137*, 084107:1−15.

(34) Maurer, M.; Ochsenfeld, C. *J. Chem. Phys.* **2013**, *138*, 174104:1−15.

(35) Ditchfield, R. *Mol. Phys.* **1974**, *27*, 789−807.

(36) Prado Ribas, F.; Giessner-Prettre, C.; Daudey, J.-P.; Pullman, A.; Hinton, J. F.; Young, G.; Harpool, D. *J. Magn. Reson.* **1980**, *37*, 431−440.

(37) Schindler, M.; Kutzelnigg, W. *J. Am. Chem. Soc.* **1983**, *105*, 1360−1370.

(38) Fukui, H.; Miura, K.; Yamazaki, H.; Nosaka, T. *J. Chem. Phys.* **1985**, *82*, 1410−1412.

(39) Hansen, A. E.; Bouman, T. D. *J. Chem. Phys.* **1989**, *91*, 3552−3560.

(40) Wolinski, K.; Hinton, J. F.; Pulay, P. *J. Am. Chem. Soc.* **1990**, *112*, 8251−8260.

(41) Malkin, V. G.; Malkina, O. L.; Salahub, D. R. *Chem. Phys. Lett.* **1993**, *204*, 87−95.

(42) Malkin, V. G.; Malkina, O. L.; Salahub, D. R. *Chem. Phys. Lett.* **1993**, *204*, 80−86.

(43) Malkin, V. G.; Malkina, O. L.; Casida, M. E.; Salahub, D. R. *J. Am. Chem. Soc.* **1994**, *116*, 5898−5908.

(44) Schreckenbach, G.; Ziegler, T. *J. Phys. Chem.* **1995**, *99*, 606−611.

(45) Schreckenbach, G.; Ziegler, T. *Int. J. Quantum Chem.* **1996**, *60*, 753−766.

(46) Schreckenbach, G.; Ziegler, T. *Int. J. Quantum Chem.* **1997**, *61*, 899−918.

(47) Lange, A.; Becker, S.; Seidel, K.; Giller, K.; Pongs, O.; Baldus, M. *Angew. Chem. Int. Ed.* **2005**, *44*, 2089−2092.

(48) de Dios, A. C.; Pearson, J. G.; Oldfield, E. *Science* **1993**, *260*, 1491−1496.

(49) Vila, J. A.; Aramini, J. M.; Rossi, P.; Kuzin, A.; Su, M.; Seetharaman, J.; Xiao, R.; Tong, L.; Montelione, G. T.; Scheraga, H. A. *Proc. Natl. Acad. Sci. U.S.A.* **2008**, *105*, 14389−14394.

(50) Vila, J. A.; Baldoni, H. A.; Scheraga, H. A. *J. Comput. Chem.* **2009**, *30*, 884−892.

(51) Arnautova, Y. A.; Vila, J. A.; Martin, O. A.; Scheraga, H. A. *Acta Crystallogr., Sect. D: Biol. Crystallogr.* **2009**, *65*, 697−703.
(52) Vila, J.; Serrano, P.; Wüthrich, K.; Scheraga, H. A. *J. Biomol. NMR* **2010**, *48*, 23−30.
(53) Martin, O. A.; Villegas, M. E.; Vila, J. A.; Scheraga, H. A. *J. Biomol. NMR* **2010**, *46*, 217−225.
(54) Chesnut, D. B.; Moore, K. D. *J. Comput. Chem.* **1989**, *10*, 648−659.
(55) Ochsenfeld, C.; Koziol, F.; Brown, S. P.; Schaller, T.; Seelbach, U. P.; Klärner, F. *Solid State Nucl. Magn. Reson.* **2002**, *22*, 128−153.
(56) Zienau, J.; Kussmann, J.; Koziol, F.; Ochsenfeld, C. *Phys. Chem. Chem. Phys.* **2007**, *9*, 4552−4562.
(57) Schaller, T.; Büchele, U. P.; Klärner, F.; Bläser, D.; Boese, R.; Brown, S. P.; Spiess, H. W.; Koziol, F.; Kussmann, J.; Ochsenfeld, C. *J. Am. Chem. Soc.* **2007**, *129*, 1293−1303.
(58) Robustelli, P.; Stafford, K. A.; Palmer, A. G., III *J. Am. Chem. Soc.* **2012**, *134*, 6365−6374.
(59) Jensen, M. R.; Salmon, L.; Nodet, G.; Blackledge, M. *J. Am. Chem. Soc.* **2010**, *132*, 1270−1272.
(60) Kjaergaard, M.; Poulsen, F. M. *Prog. Nucl. Magn. Reson. Spectrosc.* **2012**, *60*, 42−51.
(61) Ozenne, V.; Schneider, R.; Yao, M.; Huang, J.; Salmon, L.; Zweckstetter, M.; Jensen, M. R.; Blackledge, M. *J. Am. Chem. Soc.* **2012**, *134*, 15138−15148.
(62) Robustelli, P.; Kohlhoff, K.; Cavalli, A.; Vendruscolo, M. *Structure* **2010**, *18*, 923−933.
(63) Camilloni, C.; Robustelli, P.; De Simone, A.; Cavalli, A.; Vendruscolo, M. *J. Am. Chem. Soc.* **2012**, *134*, 3968−3971.
(64) Xue, Y.; Ward, J. M.; Yuwen, T.; Podkorytov, I. S.; Skrynnikov, N. R. *J. Am. Chem. Soc.* **2012**, *134*, 2555−2562.
(65) Christensen, A. S.; Sauer, S. P. A.; Jensen, J. H. *J. Chem. Theory Comp.* **2011**, *7*, 2078−2084.
(66) Christensen, A. S.; Linnet, T. E.; Borg, M.; Boomsma, W.; Lindorff-Larsen, K.; Hamelryck, T.; Jensen, J. H. Protein Structure Validation and Refinement Using Amide Proton Chemical Shifts Derived from Quantum Mechanics. http://arxiv.org/abs/1305.2164 (October 8, 2013).
(67) Kohlhoff, K. J.; Robustelli, P.; Cavalli, A.; Salvatella, X.; Vendruscolo, M. *J. Am. Chem. Soc.* **2009**, *131*, 13894−13895.
(68) Meiler, J. *J. Biomol. NMR* **2003**, *26*, 25−37.
(69) Xu, X.; Case, D. A. *J. Biomol. NMR* **2001**, *21*, 321−333.
(70) Xu, X.; Case, D. A. *Biopolymers* **2002**, *65*, 408−423.
(71) Neal, S.; Nip, A. M.; Zhang, H.; Wishart, D. S. *J. Biomol. NMR* **2003**, *26*, 215−240.
(72) Han, B.; Liu, Y.; Ginzinger, S.; Wishart, D. S. *J. Biomol. NMR* **2011**, *50*, 43−57.
(73) Shen, Y.; Bax, A. *J. Biomol. NMR* **2010**, *48*, 13−22.
(74) London, F. *J. Phys. Radium* **1937**, *8*, 397−409.
(75) Häser, M.; Ahlrichs, R.; Baron, H. P.; Weis, P.; Horn, H. *Theor. Chem. Acc.* **1992**, *83*, 455−470.
(76) Development Version of the Program Package Q-Chem. http://www.q-chem.com/ (accessed August 10, 2013).
(77) Hehre, W. J.; Ditchfield, R.; Pople, J. A. *J. Chem. Phys.* **1972**, *56*, 2257−2261.
(78) Hariharan, P. C.; Pople, J. A. *Theo. Chem. Acc.* **1973**, *28*, 213−222.
(79) Schäfer, A.; Horn, H.; Ahlrichs, R. *J. Chem. Phys.* **1992**, *97*, 2571−2577.
(80) Weigend, F.; Ahlrichs, R. *Phys. Chem. Chem. Phys.* **2005**, *7*, 3297−3305.
(81) Kollwitz, M.; Gauss, J. *Chem. Phys. Lett.* **1996**, *260*, 639−646.
(82) TURBOMOLE V6.4 2012, a Development of University of Karlsruhe and Forschungszentrum Karlsruhe GmbH, 1989−2007, TURBOMOLE GmbH, since 2007. http://www.turbomole.com (October 8, 2013).
(83) Stephens, P. J.; Devlin, F. J.; Chabalowski, C. F.; Frisch, M. J. *J. Phys. Chem.* **1994**, *98*, 11623−11627.
(84) Wilson, P. J.; Bradley, T. J.; Tozer, D. J. *J. Chem. Phys.* **2001**, *115*, 9233−9242.
(85) Keal, T. W.; Tozer, D. J. *J. Chem. Phys.* **2003**, *119*, 3015−3024.
(86) Weigend, F.; Häser, M. *Theor. Chem. Acc.* **1997**, *97*, 331−340.
(87) Weigend, F.; Häser, M.; Patzelt, H.; Ahlrichs, R. *Chem. Phys. Lett.* **1998**, *294*, 143−152.
(88) Phillips, J. C.; Braun, R.; Wang, W.; Gumbart, J.; Tajkhorshid, E.; Villa, E.; Chipot, C.; Skeel, R. D.; Kalé, L.; Schulten, K. *J. Comput. Chem.* **2005**, *26*, 1781−1802.
(89) Hornak, V.; Abel, R.; Okur, A.; Strockbine, B.; Roitberg, A.; Simmerling, C. *Proteins: Struct., Funct., Bioinf.* **2006**, *65*, 712−725.
(90) Joung, I. S.; Cheatham, T. E., III *J. Phys. Chem. B* **2008**, *112*, 9020−9041.
(91) Joung, I. S.; Cheatham, T. E., III *J. Phys. Chem. B* **2009**, *113*, 13279−13290.
(92) Case, D. A.; Cheatham, T. E., III; Darden, T.; Gohlke, H.; Luo, R.; Merz, K. M., Jr.; Onufriev, A.; Simmerling, C.; Wang, B.; Woods, R. J. *J. Comput. Chem.* **2005**, *26*, 1668−1688.
(93) Hanwell, M. D.; Curtis, D. E.; Lonie, D. C.; Vandermeersch, T.; Zurek, E.; Hutchison, G. R. *J. Cheminform.* **2012**, *4*, 1−17.
(94) Jorgensen, W. L.; Chandrasekhar, J.; Madura, J. D.; Impey, R. W.; Klein, M. L. *J. Chem. Phys.* **1983**, *79*, 926−935.
(95) Allen, M. P.; Tildesley, D. J. *Computer Simulation of Liquids*; Oxford University Press: Oxford, U.K., 1987.
(96) Martyna, G. J.; Tobias, D. J.; Klein, M. L. *J. Chem. Phys.* **1994**, *101*, 4177−4189.
(97) Feller, S. E.; Zhang, Y.; Pastor, R. W.; Brooks, B. R. *J. Chem. Phys.* **1995**, *103*, 4613−4621.
(98) Davis, I. W.; Leaver-Fay, A.; Chen, V. B.; Block, J. N.; Kapral, G. J.; Wang, X.; Murray, L. W.; Arendall III, W. B.; Snoeyink, J.; Richardson, J. S.; Richardson, D. C. *Nucleic Acids Res.* **2007**, *35*, W375−W383.
(99) Chen, V. B.; Arendall III, W. B.; Headd, J. J.; Keedy, D. A.; Immormino, R. M.; Kapral, G. J.; Murray, L. W.; Richardson, J. S.; Richardson, D. C. *Acta Crystallogr., Sect. D: Biol. Crystallogr.* **2010**, *66*, 12−21.
(100) Lovell, S. C.; Davis, I. W.; Arendall III, W. B.; de Bakker, P. I. W.; Word, J. M.; Prisant, M. G.; Richardson, J. S.; Richardson, D. C. *Proteins: Struct., Funct., Bioinf.* **2003**, *50*, 437−450.
(101) Vosko, S.; Wilk, L.; Nusair, M. *Can. J. Phys.* **1980**, *58*, 1200−1211.
(102) Lee, C.; Yang, W.; Parr, R. *Phys. Rev. B* **1988**, *37*, 785−789.
(103) Becke, A. D. *J. Chem. Phys.* **1993**, *98*, 5648−5652.
(104) Perdew, J. P. *Phys. Rev. B* **1986**, *33*, 8822−8824.
(105) Perdew, J. *P. Phys. Rev. B* **1986**, *34*, 7406.
(106) Becke, A. D. *Phys. Rev. A* **1988**, *38*, 3098−3100.
(107) Korukottu, J.; Schneider, R.; Vijayan, V.; Lange, A.; Pongs, O.; Becker, S.; Baldus, M.; Zweckstetter, M. *PLoS ONE* **2008**, *3*, e2359:1−7.
(108) Gmeiner, W. H.; Facelli, J. C. *Biopolymers* **1996**, *38*, 573−582.
(109) Havlin, R. H.; Le, H.; Laws, D. D.; de Dios, A. C.; Oldfield, E. *J. Am. Chem. Soc.* **1997**, *119*, 11951−11958.
(110) Tanuma, T.; Irisawa, J.; Ohnishi, K. *J. Fluorine Chem.* **2000**, *102*, 205−210.
(111) Zhang, Y.; Wu, A.; Xu, X.; Yan, Y. *J. Phys. Chem. A* **2007**, *111*, 9431−9437.
(112) Shen, Y.; Lange, O.; Delaglio, F.; Rossi, P.; Aramini, J. M.; Liu, G.; Eletsky, A.; Wu, Y.; Singarapu, K. K.; Lemak, A.; Ignatchenko, A.; Arrowsmith, C. H.; Szyperski, T.; Montelione, G. T.; Baker, D.; Bax, A. *Proc. Natl. Acad. Sci. U.S.A.* **2008**, *105*, 4685−4690.
(113) Martin, O. A.; Vila, J. A.; Scheraga, H. A. *Bioinformatics* **2012**, *28*, 1538−1539.
(114) Lange, A.; Giller, K.; Hornig, S.; Martin-Eauclaire, M. F.; Pongs, O.; Becker, S.; Baldus, M. *Nature* **2006**, *440*, 959−962.